Photophysical properties of meso, meso-linked porphyrin arrays: Steady-state and time-resolved fluorescence polarization

ARTICLE *in* SYNTHETIC METALS · FEBRUARY 2001

Impact Factor: 2.25 · DOI: 10.1016/S0379-6779(00)00497-5

6 AUTHORS, INCLUDING:

Dongho Kim
Yonsei University
499 PUBLICATIONS **13,545** CITATIONS

SEE PROFILE

Atsuhiro Osuka
Kyoto University
656 PUBLICATIONS **16,641** CITATIONS

SEE PROFILE

ELSEVIER

Synthetic Metals 117 (2001) 183–187

SYNTHETIC METALS

www.elsevier.com/locate/synmet

Photophysical properties of meso, meso-linked porphyrin arrays: steady-state and time-resolved fluorescence polarization

Yong Hee Kim[a], Hyun Sun Cho[a,b], Dongho Kim[a,*], Seong Keun Kim[b], Naoya Yoshida[c], Atsuhiro Osuka[c,1]

[a]*Spectroscopy Laboratory, National Creative Research Initiatives Center for Ultrafast Optical Characteristics Control, Department of Chemistry, Yonsei University, Seoul 120-749, South Korea*

[b]*Department of Chemistry, Seoul National University, Seoul 151-742, South Korea*

[c]*Department of Chemistry, Graduate School of Science, Kyoto University, Kyoto 606-8502, Japan*

Abstract

The photophysical properties of a series of directly meso,meso-linked porphyrin arrays (Zn(II) 5,15-di(3,5-di-tert-butylphenyl) porphyrin (Z1), its dimer (Z2), trimer (Z3), and tetramer (Z4), were investigated by using the steady-state and time-resolved fluorescence polarization spectroscopy. While the Soret band of Z1 exhibits the absorption maximum at 415 nm, those of Z2, Z3, and Z4 are split into two bands because of the strong exciton coupling. The fluorescence band is red-shifted and its lifetime decreases as the number of porphyrin moieties increases. In contrast to Z1, the initial anisotropy values (r_0) of Z2, Z3 and Z4 exhibit the negative sign with photoexcitation at 410 nm, indicating a large difference between absorption and emission dipole orientations. However, the positive values are obtained in all compounds with the visible excitation. The emission anisotropy decay appeared to be monoexponential at all excitation wavelengths with a decrease of its rate as the number of porphyrin moieities increases. In addition, the rotational decay is observed to depend on excitation wavelength, which is probably due to the local heating of the solvent by excess vibrational energy. The anisotropy values calculated from the time-resolved anisotropy decay are in a good agreement with those obtained from the steady-state polarized excitation spectra.

Keywords: Directly meso, meso-linked porpyrin arrays; Anisotropy; Absorption and emission spectroscopy; Excitation polarization spectroscopy; Time-resolved fluorescence polarization spectroscopy

1. Introduction

The various types of covalently linked arrays of metalloporphyrins have been designed and synthesized with the goal of applying the molecular oligomers to molecular photonic devices and artificial biomimetic light-harvesting arrays [1]. In addition to achieving highly efficient energy transfer, such systems must possess organic solubility and architectural rigidity and allow the incorporation of many porphyrinic pigments in precise states of metalation and geometrical arrangement. Since the preparation and purification of molecular assembly is indeed an intensive labor-consuming work, the ability to reliably predict the performance characteristics of aimed molecular photonic devices is highly desirable. There has been a great advance in synthesizing numerous multi-porphyrin light-harvesting array architectures especially with distinct linkage interconnecting porphyrin molecular species [2]. Multi-porphyrin arrays have been constructed using several types of shorter linkers that are suitable for preparing linear or extended architectures via meso position attachment [3]. The recent progress in synthesizing capabilities of various porphyrin arrays raises a fundamental question regarding the photophysical properties and molecular architecture relationship, such as energy migration/gradient. The numbers of pigments, electronic properties of pigments, and linkage structure have a strong influence on the overall photophysical properties of porphyrin oligomers [4].

Especially the exciton coupling strength mainly governed by the interconnection length between porphyrin molecules is one of the most distinct phenomena occurring in molecular assembly. These interactions are more significant in the Soret region due to the large transition dipole moment associated with these transitions and are manifest in the pronounced spectral splitting over 400–500 nm energy domain [5].

* Corresponding author.
[1] Co-corresponding author.

0379-6779/01/$ – see front matter
PII: S0379-6779(00)00497-5

Furthermore, the direct meso–meso connection results in stronger electronic coupling to exhibit further split Soret band. But the Q bands of these porphyrin arrays are much less perturbed due to poor electronic communication imposed by the orthogonality of the adjacent porphyrins. In order to investigate the photophysical properties of directly linked (porphinato)-zinc(II) systems, it is important to consider the range of sterically accessible chromophore–chromophore dihedral angles at ambient temperature and the porphyrin-to-porphyrin linkage topology in the ground and excited states.

With these objectives in this investigation, the directly linked zinc(II) porphyrin dimer, trimer, and tetramer along with their corresponding monomer are employed to investigate the difference in the exciton coupling dynamics accompanied by the relative orientational motion between the two porphyrin rings. For a systematic approach, we have performed steady-state absorption, emission, and anisotropy measurements to have structural information of these porphyrin oligomers. The fluorescence anisotropy decay was conducted to explore rotational diffusion related to molecular structure along with the decay of the lowest excited emitting state.

2. Experimental

The (Zn(II) 5,15-di(3,5-di-tert-butylphenyl) porphyrin (Z1), its meso,meso-linked porhyrin dimer (Z2), trimer (Z3), and tetramer (Z4) were synthesized [5]. The spectroscopic grade tetrahydrofuran solvent was used for all experiments.

The absorption spectra were recorded by using a Varian Cary 3 spectrophotometer. The fluorescence measurements were made on a scanning SLM-AMINCO 4800 spectrofluorometer, which makes possible to obtain the corrected spectrum using rhodamine B as a quantum counter. Polarization dependent emission was detected by using the polarizers, placed in the excitation and emission path. Excitation anisotropy (r) spectrum could be obtained by measuring the G factor of the instrument [6].

The picosecond time resolved fluorescence experiments were carried out by using time correlated single photon counting (TCSPC) method. The picosecond excitation pulses at 563 nm were obtained from a cavity-dumped picosecond dye laser (Coherent 702) synchronously pumped by a mode-locked Ar ion laser (Coherent Innova 200). The cavity dumped beam from the dye laser has 2 ps pulse width and an average power of ca. 40 mW at 3.8 MHz dumping rate when rhodamine 6 G for gain dye was used. The excitation pulses at 410 nm were obtained from a femtosecond Ti:Sappahire laser with an average power of 600 mW at 820 nm. The pump pulses at desired wavelength were generated by frequency doubling with a β-BBO crystal. The emission was collected at 45° angle with respect to the excitation laser beam by 5 and 25 cm focal length lenses, focused onto a monochromator (Jovin–Yvon HR320), and detected with a microchannel plate photomultiplier tube (Hamamatsu R2809U). The signal was amplified by a wide-band amplifier (Philip Scientific), sent to a Quad constant fraction discriminator (Tennelec), a time-to-amplitude converter (Tennelec), a counter (Ortec), and a multichannel analyzer (Tennelec/Nucleus), and stored in a computer.

3. Results and discussion

Fig. 1 shows the structures of porphyrin monomer and its arrays which are directly linked at their respective meso-carbon positions.

Fig. 2 shows the absorption spectra of monomeric, dimeric, trimeric and tetrameric porphyrins (Z1, Z2, Z3, and Z4) in THF, which display the interesting systematic changes in the Soret (B) bands with an increase in the number of porphyrin moieties. While the Soret band of Z1 exhibits the absorption maximum at 415 nm, that of Z2 is split into two bands with absorption peaks at 421 and 457 nm. The splitting of the Soret band becomes more significant as the number of porphyrin moieties increases. The splitting energies of the Soret band are observed to be 1871, 3220 and 3594 cm^{-1} in Z2, Z3, and Z4, respectively, indicating that the electronic states of Z2, Z3, and Z4 are increasingly perturbed compared to monomeric porphyrin (Z1), as expected from the splitting of B band and the relative ratio of B band to Q band intensity. Also the absorption bandwidths of Z2, Z3, and Z4 are much broader than that of Z1, which may reflect the inhomogeneity due to

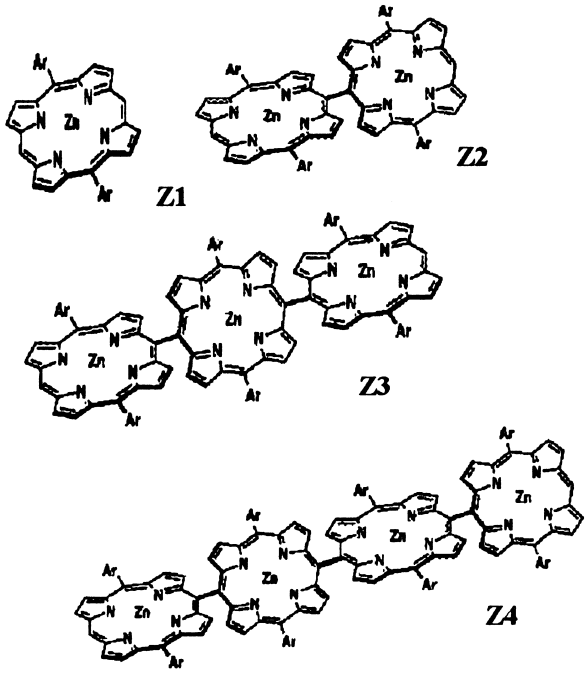

Fig. 1. The structures of Z1, Z2, Z3, and Z4, where Ar represents 3,5-ditertbutylphenyl.

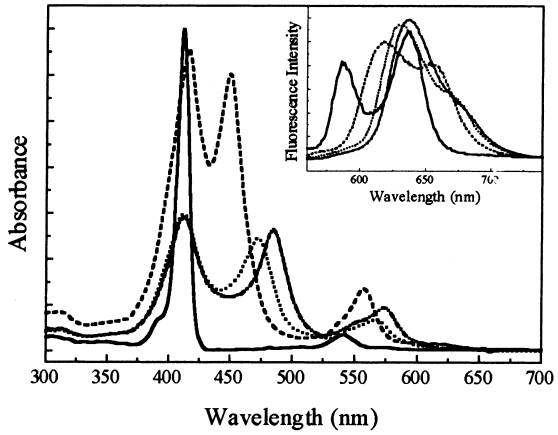

Fig. 2. Absorption and emission spectra (inset) of Z1 (—); Z2 (- - -); Z3 (. . .); and Z4 (-·-·-·) in THF.

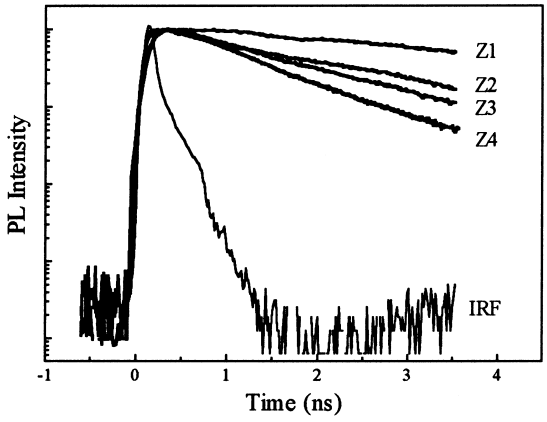

Fig. 3. The fluorescence decay profiles of Z1–Z4.

the conformers with a dihedral angle distribution between adjacent porphyrin moieties. MNDO calculation indicates that the potential energy surface in the dihedral angle range of 80–90° is at minimum energy in Z2, Z3, and Z4.

The systematic change of the splitting energy can be explained in terms of exciton coupling theory [7,8]. According to the exciton coupling theory, the transition dipole moments residing in each moiety interact electrostatically to create two exciton states, Ψ^+ and Ψ^-. The Ψ^+ state corresponds to the situation where both monomeric units are excited in phase. For Ψ^- state, both monomers are out of phase.

The absorption frequencies of the transitions depend on the angle between the transition dipoles and the relative phase of their excitations. For oligomers the transition moment can be computed by adding each individual transition dipole vectorically and its intensity can be obtained by computing the square of the length of the resulting vector. The exciton coupling is expected to be strong in directly meso-linked arrays because of the short interconnection between porphyrin moieties. However, the exciton coupling strength is not so large as much as expected, indicating the porphyrin moieties are distorted with a considerable angle distribution. The Q bands in absorption spectra show a small energy splitting regardless of the presence of strong perturbation between porphyrin moieties, demonstrating their small dipole moments compared to those of B bands. The Q band seems to be red-shifted and its splitting is slightly enhanced by increasing the porphyrin moieties.

The fluorescence emission spectrum of Z1 exhibits the vibronic emission bands at 587 and 637 nm (inset of Fig. 2). The emission bands are red-shifted with an increase in the number of porphyrin moieties as expected. We have measured the fluorescence decay profiles at various wavelengths with excitations at B and Q bands, showing no dependence on excitation and emission wavelengths. The decay profiles following the photoexcitation at Q band are shown in Fig. 3. As the number of porphyrin moieties increases, the fluorescence lifetime decreases (Table 1). The measured lifetime

Table 1
Fluorescence and anisotropy decay parameters

Compounds	λ_{ex}[a]	λ_{em}[b]	τ (ns)[c]	r_0[d]	Φ (ns)[e]	δ[f]	r[g]
Z1	560	586	2.57	0.23	0.3	32	0.025 (0.023)[a]
	410			0.13	0.2	42	0.01 (0.018)
Z2	563	618	1.93	0.19	0.5	36.4	0.03 (0.028)
	410			−0.05	0.43	60	−0.01 (−0.015)
Z3	568	632	1.58	0.19	0.7	36	0.06 (0.064)
	410			−0.18	0.64	63	−0.03 (−0.03)
Z4	575	634	0.92	0.28	1.1	26	0.15 (0.13)
	410			−0.03	1.0	58	−0.01 (−0.03)

[a] Excitation wavelength.
[b] Emission wavelength.
[c] Fluorescence lifetime.
[d] Initial anisotropy at $t = 0$.
[e] Anisotropy decay time.
[f] Angle between the absorption and emission dipoles.
[g] Anisotropy estimated from steady-state polarized excitation spectra.

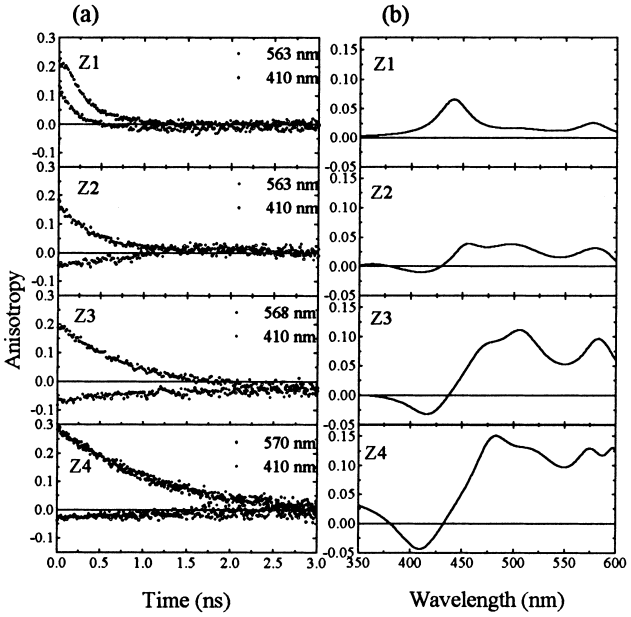

Fig. 4. (a) Fluorescence anisotropy decay profiles of Z1–Z4, following the B and Q band photoexcitations. (b) Steady-state excitation anisotropy spectra.

of the excited state reflects both radiative and nonradiative pathways, $k = k_{fl} + k_{ISC} + k_{IC}$, where k_{fl}, k_{ICS}, and k_{IC} are the fluorescence decay, intersystem crossing, and internal conversion rates, respectively.

Thus, as the nonradiative relaxation becomes important the fluorescence lifetime becomes increasingly shorter. In a large molecule with a higher density of states, the fluorescence decays more rapidly via nonradiative relaxation processes such as intersystem crossing (IC) and internal conversion (ISC). In order to get information on the orientations of transition dipoles and the anisotropic behaviors of Z1–Z4, we have measured the polarized fluorescence excitation spectra and the time-resolved anisotropy decay. The emission anisotropy decay profiles for Z1–Z4 in THF are shown in Fig. 4. The excitation wavelengths were B band (410 nm) and Q band (563 nm), and the emission wavelengths were 586, 618, 632, and 634 nm for Z1, Z2, Z3, and Z4, respectively. The r_0 values of porphyrin arrays are dependent on the excitation wavelength. Different r_0 values result from the orientational change between the absorption and emission transition dipoles. According to Kasha's rule, the lowest singlet excited state is responsible for the fluorescence regardless of the initially populated state in the aromatic compounds.

Therefore, the excitation energy dependent anisotropy (r_0) can be suggested to result from the change in absorption dipole. The r_0 values in Z2–Z4 exhibit the negative sign with an excitation at 410 nm, whereas positive with an excitation at Q band, which implies that the absorption transition dipole characteristics of two bands are very different. However, r_0 values in Z1 are all positive, indicating no significant change in the transition dipole orientation between absorption and emission. For B band excitation of Z2–Z4, the absorption dipole is aligned with a large angle to emission dipole. This suggests that the transition dipole in arrays is enhanced along the long axis. Based on the initial value (r_0) of the time-resolved anisotropy data, the angle δ between absorption and emission dipoles can be estimated from the limiting emission anisotropy $r_0 = 0.2(3\cos^2\delta - 1)$ (Table 1). We have also calculated the anisotropy values (r) using the Perrin equation

$$r = \frac{r_0}{1 + (\tau/\Phi)}$$

where r_0, Φ, and τ are the initial anisotropy value, the anisotropy decay time, and the fluorescence lifetime, respectively. The fluorescence anisotropy decays ($r(t)$) offer the detailed information on the diffusive motions of the fluorophore. It is well known that $r(t)$ exhibits multi-exponential decay rates due to anisotropic rotations with respect to molecular coordinates. If we approximate the molecular shape as a sphere the fluorescence anisotropy decays monoexponentially with its decay rate proportional to rotational diffusion rate. The slower fluorescence anisotropy decay could be expected for larger molecules because of the inertial momentum and friction by surrounding solvents. As seen in Fig. 4(a) and Table 1, the fluorescence anisotropy decay rates decrease with an increase in the number of porphyrin moieties.

More specifically, one may expect in-plane rotations of porphyrin to be more rapid than out-of-plane ones because the shape of porphyrin monomer is like a disk. The out-of-plane motion must displace the plane of the molecule spatially, which requires more energy than in-plane motions. The in-plane rotations probably require less displacement of solvent and thus, expected to be more rapid. The decay of the emission anisotropy appeared to be monoexponential at all excitation wavelengths, which means that it may be dominated by a major rotational motion. The most probable candidate is the rotational motion along the long axis. That is, upon increasing the number of porphyrin moieties, the overall molecular shape of these oligomers become elongated in the direction of the addition of porphyrin moieties. On the contrary, the in-plane rotational contributions to the overall rotational diffusion motion are less significant upon increasing the number of porphyrin units. The anisotropy values calculated from the time-resolved anisotropy decay are in agreement with the steady-state polarized excitation spectra data shown in Fig. 4(b). The polarization excitation spectra indicate that the dipole orientations strongly depend on the excitation wavelengths. It is noteworthy that the rotational orientational times depend on excitation wavelength. The anisotropy decay time is shorter as the excitation energy increases. These results could be explained by the local heating of the solvent arising from the excess vibrational energy.

In summary, the exciton splitting of Z1–Z4 becomes larger as the number of porphyrin moieties increases. The

absorption bandwidths of Z2–Z4 are much broader than that of Z1 due, in some parts, to the conformational inhomogeneity. The fluorescence decay becomes faster while the rotational diffusion motion becomes slower as the number of porphyrin moieties increases. The directly meso,meso-linked porphyrin arrays exhibit the topological inhomogeneity, which has an influence on the exciton coupling dynamics. Therefore, it is important to consider the structural and electronic effects on the exciton coupling and energy migration in designing the artificial light harvesting arrays and the molecular electronic devices based on multi-porphyrin molecular arrrays.

Acknowledgements

This work has been financially supported by the National Creative Research Initiatives of the Ministry of Science & Technology of Korea. The work at Kyoto was supported by Grant-in-Aids for Scientific Research from the Ministry of Education, Science, Sports and Culture of Japan and by CREST (Core Research for Evolutional Science and Technology) of Japan Science and Technology Corporation (JST).

References

[1] V.S.–Y. Lin, S.G. DiMagno, M.J. Therien, Science 264 (1994) 1105.
[2] R.W. Wagner, J.S. Lindsey, V. Palaniappan, D.F. Docian, J. Am. Chem. Soc. 118 (1996) 3996.
[3] A. Osuka, S. Marumo, N. Mataga, S. Taniguchi, T. Okada, I. Yamazaki, Y. Nishimura, T. Ohno, K. Nozaki, J. Am. Chem. Soc. 118 (1996) 155.
[4] .A. Osuka, K. Maruyama, J. Am. Chem. Soc. 110 (1988) 4454.
[5] A. Osuka, H. Shimidzu, Angew. Chem. Int. Ed. Engl. 36 (1997) 135.
[6] J.R. Lakowicz, Principles of fluorescence spectroscopy, Plenum Press, New York, 1983.
[7] M. Kasha, H.R. Rawls, M.A. El-Bayoumi, Pure Appl. Chem. 11 (1965) 371.
[8] G.A. Schick, I.C. Schreiman, R.W. Wagner, J.S. Lindsey, D.F. Bocian, J. Am. Chem. Soc. 111 (1989) 1344.